

Mobilization of Protein Kinase C in Macrophages Induced by *Listeria monocytogenes* Affects Its Internalization and Escape from the Phagosome

Sandra J. Wadsworth† and Howard Goldfine*

Department of Microbiology, University of Pennsylvania School of Medicine, Philadelphia, Pennsylvania 19104-6076

Received 26 December 2001/Returned for modification 11 March 2002/Accepted 19 April 2002

Listeriolysin O (LLO) and a phosphatidylinositol-specific phospholipase C (PI-PLC) are known virulence factors of *Listeria monocytogenes* in both tissue cultures and the murine model of infection. LLO is a member of a family of pore-forming cholesterol-dependent cytotoxins and is known to play an essential role in escape from the primary phagocytic vacuole of macrophages. PI-PLC plays an accessory role, in that PI-PLC mutants are partially defective in escape. We have shown that both of these molecules are essential for initiating rapid increases in the calcium level in the J774 murine macrophage cell line (S. J. Wadsworth and H. Goldfine, Infect. Immun. 67:1770-1778, 1999). Here we show that both LLO and PI-PLC are required for translocation of protein kinase C δ (PKC δ) to the periphery of J774 cells and for translocation of PKC β II to early endosomes beginning within the first minute after addition of bacteria to the culture medium. Treatment with the calcium channel blocker SK&F 96365 inhibited translocation of PKC β II but not PKC δ . Our findings lead us to propose a host signaling pathway requiring LLO and the formation of diacylglycerol by PI-PLC in which calcium-independent PKC δ is responsible for the initial calcium signal and the subsequent PKC β II translocation. LLO-dependent translocation of PKC β I to early endosomes also occurs between 1 and 4 min after infection, but this occurs in the absence of PI-PLC. All of these signals were observed in cells that had not internalized bacteria. Blocking PKC β translocation with hispidin resulted in more rapid uptake of wild-type bacteria and greatly reduced escape from the primary phagocytic vacuoles of J774 cells.

The capacity to survive and grow within macrophages is a hallmark of infections with *Listeria monocytogenes*. Our recent studies have focused on the earliest stages of the encounter between *L. monocytogenes* and a macrophage, as represented by the J774 murine macrophage cell line, a well-studied tissue culture model of infection (5, 30, 33). We have observed that the cytosolic calcium level is elevated at 1, 5, and 10 min after infection with wild-type *L. monocytogenes* but not after infection with a strain with a listeriolysin O (LLO) mutation. Strains with deletions in the genes encoding two secreted phospholipases C did not produce some or all of these signals (35).

Of specific interest to workers in our laboratory are signal transduction pathways activated by the two phospholipases that contribute significantly to virulence in the mouse model of infection (5, 30). One of these, a phosphatidylinositol (PI)-specific phospholipase C (PI-PLC), encoded by *plcA*, hydrolyzes host PI, leading to production of the eukaryotic signaling molecule diacylglycerol (DAG) (4, 12, 23, 30). The other, a broad-range phospholipase C (BR-PLC), encoded by *plcB*, acts on many host polar lipids, including sphingomyelin, leading to production of DAG and ceramide (10, 11). The elevated calcium levels produced by the combined actions of LLO and PI-PLC appear to be part of a signaling pathway that is inhibitory to entry of *L. monocytogenes*, since strains with mutations

in the genes encoding these two proteins enter J774 cells more rapidly than the wild type enters these cells (35). Calcium signals also appear to regulate the eventual fate of the bacterium since suppression of these signals results in more rapid entry and reduced escape of wild-type bacteria from the primary phagocytic vacuole into the cytosol (35).

Based on the rapid hydrolysis of PI and the formation of DAG as a result of listerial phospholipase activity on host lipids (12) and based on our observations of calcium signaling (35), we investigated the possibility that calcium signaling is coupled to protein kinase C (PKC) mobilization. In the present study we demonstrated that three of the four PKC isoforms (δ , β I, and β II) found in J774 cells are translocated before bacterial entry, that the presumed activation of PKC δ and PKC β II is coupled to early calcium signals, and that both β isoforms rapidly translocate to early endosomes. Pharmacological inhibition of PKC signaling resulted in more rapid entry and reduced escape of *L. monocytogenes* from the primary phagocytic vacuole.

MATERIALS AND METHODS

Bacterial strains and culture conditions. Bacterial strains used in this study are listed in Table 1. All strains were maintained on brain heart infusion agar plates, which were made at regular intervals from stock cultures stored at -80°C in Luria-Bertani medium with 40% glycerol. For all experiments an overnight culture was grown statically at 30°C , and a 1:10 dilution of this culture in brain heart infusion was prepared the morning of the experiment and grown at 37°C on a rotator until the optical density at 620 nm reached 0.490 to 0.510.

Measurement of bacterial association with and entry into J774 cells. J774 cells, a murine macrophage cell line, were maintained in Dulbecco's modified Eagle's medium (DMEM) supplemented with 7.5% fetal calf serum, glutamine, and penicillin-streptomycin and incubated at 37°C under 5% CO_2 . Cells were plated on circular glass coverslips (diameter, 12 mm; Fisher) in antibiotic-free

* Corresponding author. Mailing address: Department of Microbiology, University of Pennsylvania School of Medicine, Philadelphia, PA 19104-6076. Phone: (215) 898-6384. Fax: (215) 898-9557. E-mail: goldfinh@mail.med.upenn.edu.

† Present address: Department of Pharmacology, Temple University School of Medicine, Philadelphia, PA 19140-5104.

TABLE 1. *L. monocytogenes* strains used in this study

Strain ^a	Genotype	Phenotype	Reference
10403S	Wild type		25
DP-L1552	$\Delta plcA$	PI-PLC ⁻	5
DP-L1935	$\Delta plcB$	BR-PLC ⁻	30
DP-L1936	$\Delta plcA \Delta plcB$	PI-PLC ⁻ BR-PLC ⁻	30
DP-L2161	Δhly	LLO ⁻	15

^a All mutants are in-frame deletion mutants of strain 10403S.

DMEM 1 day prior to infection. To measure entry, we used the method of Drevets and Campbell (8). Briefly, cells were infected with fluorescein isothiocyanate (FITC)-labeled log-phase wild-type or mutant bacteria (25 to 30 bacteria per cell) for 20 min. Bacteria were labeled with FITC as described previously (35). At various times during the 20-min infection period cells were washed five or six times with phosphate-buffered saline (PBS), stained with ethidium bromide (25 μ g/ml), which stains only extracellular bacteria, and fixed with 3.3% formaldehyde. Cells and bacteria were counted by using a 60 \times oil objective and both fluorescein and rhodamine filters. Total bacteria, stained with FITC, were green, and extracellular bacteria, stained with ethidium bromide, were red. Thus, the percentage of intracellular bacteria was obtained by subtracting the number of extracellular bacteria (red) from the number of total bacteria (green), dividing the difference by the total number of bacteria (green), and multiplying this fraction by 100 (35).

Visualization of PKC translocation by immunofluorescence. Immunofluorescence techniques were used to study PKC δ and PKC β translocation and colocalization of PKC β with early endosomes of J774 cells. For these studies, cells were plated on coverslips as described above. Cells were infected with FITC-labeled wild-type or mutant bacteria, and at various times during a 5-min infection cells were washed five or six times with PBS, fixed, permeabilized with PBS containing 0.1% Triton X-100, and blocked with 1% bovine serum albumin. In some experiments unlabeled bacteria were used to determine if FITC labeling altered the signals obtained with labeled bacteria. No difference in signaling was seen when labeled and unlabeled bacteria were compared. The permeabilized cells were then incubated at 37°C for 1 h with rabbit polyclonal antibodies (1:100) to murine PKC δ , PKC β I, or PKC β II (Calbiochem, San Diego, Calif.). Then the cells were washed 10 times with PBS, the secondary antibody, anti-rabbit immunoglobulin G conjugated to FITC, was added at 1:100, and the cells were incubated for 30 min at 25°C. After this incubation the cells were washed 10 times with PBS and mounted for fluorescence microscopy. Cells were viewed with the 60 \times oil objective by using the fluorescein filter.

In experiments in which PKC β colocalization to early endosomes was studied, J774 cells were also labeled with rhodamine-conjugated transferrin (Molecular Probes), a specific marker for early endosomes. J774 cells were labeled for 45 min at 37°C with transferrin according to the manufacturer's directions, washed 10 times with PBS, and then infected with wild-type or mutant bacteria. The cells were then processed for immunofluorescence studies as described above. These cells were viewed with both the fluorescein and rhodamine filters.

Cytosolic Ca²⁺ measurements. Cytosolic calcium measurements were obtained as previously described (35). Briefly, cells were loaded with a 5 μ M solution of the fluorescent calcium indicator fluo-3 AM and a 5 μ M solution of the fluorescent indicator SNARF-1 AM for 30 min. SNARF-1 AM was used as the reference since fluo-3 is a nonratiometric calcium indicator. The cells were viewed with a 40 \times objective by using both fluorescein and rhodamine filters, and dual images were captured with the Phase 3 Imaging system (Phase 3 Imaging, Glen Mills, Pa.).

Early-endosome preparation and characterization: isolation of early endosomes. Early endosomes were isolated and characterized by the methods of Diaz et al. (7), with modifications. J774 cells, grown to confluence in 150-cm² flasks, were infected with *L. monocytogenes* and washed three times with ice-cold PBS. Bacterial cultures were not labeled with FITC but otherwise were prepared as described above. The volume of inoculum required varied according to the number of flasks of J774 cells used but was calculated based on a multiplicity of infection of 25 to 30. Immediately after the last wash liquid was removed, 3 ml of ice-cold lysis buffer (10 mM Tris, 1 mM diisopropyl fluorophosphate, 0.5 μ g of leupeptin per ml, 2 μ g of aprotinin per ml, 1 mM phenylmethylsulfonyl fluoride, 1 mM dithiothreitol, 1 mM EGTA, 1 mM EDTA; pH 7.4) was added to each flask, and the cells were immediately scraped, transferred into a 15-ml conical polypropylene tube (Costar), and kept on ice. The cell suspension was incubated for approximately 5 min on ice or until more than 85% of the cells were lysed, as determined by microscopy. The suspension was centrifuged for 5 min at 1,500

$\times g$ at 4°C. The postnuclear supernatant (PNS) fraction was collected, transferred to an SW41 ultracentrifuge tube (Beckman), and centrifuged for 15 min at 40,000 $\times g$ at 4°C. The supernatant (first supernatant fraction) was collected and saved for marker assays. The pellet was resuspended in 0.25 ml of 0.25 M sucrose in lysis buffer; for the best results, we applied the 40,000- $\times g$ pellet obtained from four 150-cm² flasks to one Percoll gradient. This suspension was then layered onto 1.5 ml of a 1.05-g/ml Percoll solution. It was centrifuged for 45 min at 40,000 $\times g$ in the SW41 rotor, and the early-endosome fraction was collected from the top of the tube and used for marker assays or Western blotting. The thin lipid layer, located below the early-endosome fraction, was discarded, and the aqueous layer below this was referred to as late endosomes/lysosomes. This layer was also saved and was used for marker assays.

Transferrin receptor detection. Early endosomes were prepared as described above, the five fractions obtained from the preparation were loaded onto a sodium dodecyl sulfate (SDS)-10% polyacrylamide gel, and the proteins were separated by electrophoresis. Proteins were then transferred to polyvinylidene difluoride membranes (Bio-Rad), and Western immunoblotting was performed by using a monoclonal anti-transferrin receptor antibody. The transferrin receptor was found in the PNS fraction which was the starting material for the isolation, the 40,000- $\times g$ pellet obtained after 15 min of ultracentrifugation, and the purified early-endosome fraction. No bands were detected in the first supernatant or the late-endosome/lysosome fraction (data not shown).

HRP assay. Five separate preparations of early endosomes isolated from J774 cells were characterized with respect to horseradish peroxidase (HRP) activity (1). One confluent 150-cm² flask of J774 cells (20 $\times 10^8$ to 30 $\times 10^8$ cells) was incubated for 1 h at 4°C with 200 μ g of HRP-avidin conjugate (Sigma, St. Louis, Mo.) per ml. Uptake of the conjugated probe was initiated by addition of prewarmed (37°C) tissue culture medium (without marker), and the pulse-chase reaction was stopped after 10 min by addition of ice-cold PBS. After incubation for 10 min at 37°C, the HRP-avidin marker is located in the early endosomes (18). Cells were washed three times with ice-cold PBS, and then the early endosomes were isolated as described above. The five fractions described above were analyzed for HRP activity by the method of Alvarez-Dominguez et al. (1); *o*-dianisidine was used as the substrate. A calibration curve (0 to 50 ng of HRP-avidin) was used to quantify the concentration of the marker in each fraction.

In a second set of three preparations J774 cells were loaded with HRP-avidin as described above, except that the reaction was stopped with ice-cold PBS after 45 min rather than after 10 min. The additional incubation time allowed the HRP marker to pass through the early endosomes and enter the late endosomes and lysosomes (6). The fractions described above were assayed for HRP-avidin activity.

***N*-Acetyl- β -D-glucosaminidase assay.** *N*-Acetyl- β -D-glucosaminidase, a lysosomal enzyme, was assayed by the method of Findlay et al. (9). This enzyme catalyzes hydrolysis of the substrate *p*-nitrophenyl-*N*-acetyl- β -D-glucosaminide, yielding free *p*-nitrophenol. Briefly, 0.5 ml of sample was added to 1 ml of 0.2 N citric acid buffer (pH 4.4) and 2 ml of 10 mM *p*-nitrophenyl-*N*- β -D-glucosaminide. After incubation for 1 h at 38°C, the reaction was stopped by addition of 4 ml of 0.4 M glycine-NaOH buffer (pH 10.5). The reaction mixture was centrifuged at 3,000 $\times g$, and the amount of *p*-nitrophenol in the supernatant was determined by measuring absorbance at 430 nm. Specific activity was expressed in absorbance units per milligram of protein. Total activity was expressed in absorbance units per milligram of protein in the whole preparation.

Western blotting for PKC β I and PKC β II colocalization with isolated early endosomes. J774 cells were maintained in DMEM with 7.5% fetal calf serum and antibiotics in 150-cm² flasks at 37°C under 5% CO₂. One day prior to infection the cells were switched to antibiotic-free DMEM with 7.5% fetal calf serum. Log-phase bacterial cultures were grown as described above. For PKC β I and early-endosome colocalization, 12 $\times 10^9$ to 15 $\times 10^9$ cells were used for each infection; the same number of cells was used for the uninfected control. PKC β II colocalization with early endosomes required 16 $\times 10^9$ to 18 $\times 10^9$ cells per infection or for the uninfected control. To isolate early endosomes colocalized with PKC β I, cells were infected with wild-type or mutant *L. monocytogenes* at 37°C at a multiplicity of infection of 25 for 4 min (the time of maximal colocalization, as determined by immunofluorescence studies), washed three times with ice-cold PBS, and processed as described above for isolation of early endosomes. For isolation of early endosomes colocalized with PKC β II, cells were infected with wild-type or mutant *L. monocytogenes* at 37°C for 45 s (the time of maximal colocalization, as determined by immunofluorescence) and processed for early-endosome isolation.

The purified fractions (100 μ g of protein) were applied to SDS-10% polyacrylamide gels. After electrophoresis and transfer to polyvinylidene difluoride membranes, Western immunoblotting was performed by using primary PKC

TABLE 2. Characterization of early endosomes

Fraction	Sp act	Total activity	% Activity
HRP assay ^a			
PNS	2,080 ± 372	6,250 ± 1,120	(100)
First supernatant	280 ± 52	830 ± 156	14 ± 3.0
Pellet	9,180 ± 2,633	4,590 ± 1,316	70 ± 16
Early endosomes (10-min pulse)	11,090 ± 1,832	5,800 ± 955	96 ± 12
Late endosomes/lysosomes (10-min pulse)	230 ± 48	400 ± 93	6.7 ± 1.6
Early endosomes (45-min pulse)	150 ± 86	80 ± 43	0.90 ± 0.40
Late endosomes/lysosomes (45-min pulse)	3,850 ± 1360	5,770 ± 2,040	80 ± 11
<i>N</i> -Acetyl-β-D-glucosaminidase assay ^b			
PNS	2.20 ± 0.25	6.70 ± 0.74	(100)
First supernatant	0.067 ± 0.04	0.20 ± 0.12	3.3 ± 2
Pellet	13.0 ± 7.2	6.7 ± 3.6	94 ± 40
Early endosomes	0.09 ± 0.11	0.05 ± 0.05	0.7 ± 0.9
Late endosomes/lysosomes	2.90 ± 0.72	4.30 ± 1.1	60 ± 15

^a The HRP assay for five fractions was performed as described in text. The specific activity of the marker was calculated for each preparation and is expressed in nanograms of HRP-avidin per milligram of protein, and the average total activity is expressed in nanograms of HRP-avidin per milligram of protein in the total volume. The PNS fraction activity was considered 100%, and the percentage of activity for each of the remaining fractions was determined as follows: total activity in fraction/total activity in PNS fraction. The data are means ± standard errors for five separate preparations.

^b The *N*-acetyl-β-D-glucosaminidase assay for five fractions was performed as described in text. The specific activity is expressed in absorbance per milligram of protein. The PNS fraction activity was considered 100%, and the percentage of activity for each of the remaining fractions was determined as follows: total activity in fraction/total activity in PNS fraction. The data are means ± the standard errors for five separate preparations.

antibodies at a dilution of 1:500 for 1 h and rabbit anti-immunoglobulin G secondary antibody conjugated to HRP at a dilution of 1:10,000 for 1 h. Blots were developed with the Super Signal chemiluminescence system (Pierce, Rockford, Ill.).

RESULTS

Characterization of the early-endosome preparation. The early-endosome preparation was characterized by measuring the activities of three subcellular markers in different fractions of the preparation, as described in Materials and Methods and summarized in Table 2. In five preparations in which J774 cells had been given a 10-min pulse of the endocytic marker HRP, the HRP activity was completely recovered in the top fraction of the Percoll gradient, indicating that this fraction contained the purified early-endosome fraction. A Western blot showed that the PNS fraction, the first pellet, and the top fraction of the Percoll gradient also contained the early endosomal transferrin receptor marker (data not shown). The Western blot thus confirmed that the top fraction of the gradient contained the purified early-endosome fraction. HRP activity was also measured in a second set of three preparations after a 45-min HRP pulse, during which HRP was expected to progress to late endosomes or lysosomes (6). There was no significant HRP activity remaining in the early-endosome fraction, indicating that this fraction was not contaminated with late endosomes or lysosomes. The activity of the lysosomal marker, *N*-acetyl-D-glucosaminidase, was measured, and no significant glucosaminidase activity was detected in the early-endosome fraction, indicating that this fraction was free of lysosomal contamination.

Translocation of PKC after infection with wild-type and mutant *L. monocytogenes*. (i) **PKC δ translocation.** Addition of wild-type *L. monocytogenes* or the strain lacking the BR-PLC (data not shown) to J774 cells caused rapid redistribution of PKC δ from the diffuse cytoplasmic signal seen in uninfected cells (Fig. 1A, panel a), which resulted in peripheral localization (Fig. 1A, panel c) or clusters near the periphery (Fig. 1A,

panel d). Similar translocation was observed after treatment with phorbol myristate acetate (PMA), an activator of PKC (Fig. 1A, panel b). The observed redistribution began 30 s after addition of either strain to cell cultures and reached a maximum by 45 s. By 5 min PKC δ had redistributed to a cytosolic location (data not shown). Infection with the PI-PLC mutant (Fig. 1A, panel f), the LLO mutant (Fig. 1A, panel e), or double phospholipase mutants ($\Delta plcA \Delta plcB$) (data not shown) did not result in redistribution of PKC δ, indicating that both LLO and PI-PLC are required for PKC δ translocation.

(ii) **Effects of inhibitors on PKC δ translocation.** Although it has been reported that PKC δ activation is calcium independent, the effects of the calcium channel blocker SK&F 96365 on PKC δ translocation have not been examined. We tested SK&F 96365 (BioMol) at a concentration of 25 μM, the concentration previously shown to completely inhibit calcium signaling in J774 cells (35), and we found that it did not affect translocation of PKC δ after infection with the wild type (Fig. 1B, panels c and d). Hispidin (Calbiochem), a potent inhibitor of PKC β isoforms (50% inhibitory concentration, 2 μM) (13), was also tested to determine its effects on PKC δ activity. PKC δ translocation was not affected by 5 μM hispidin, the concentration that resulted in complete inhibition of PKC β I and PKC II translocation to early endosomes (see below) (Fig. 1B, panels e and f). Rottlerin (Calbiochem), a relatively specific inhibitor of PKC δ (14, 17), completely inhibited translocation at a concentration of 25 μM (Fig. 1B, panels g and h).

(iii) **PKC β II translocation.** Using epifluorescence and Western immunoblotting, we observed that PKC β II translocated to early endosomes after infection with the wild type. In uninfected cells PKC β II was distributed throughout the cell and also colocalized with early endosomes (Fig. 2a to c). The cells in Fig. 2a to c are representative of the population of uninfected cells in which ≤10% colocalization of PKC β II with early endosomes was routinely observed. Colocalization of PKC β II with an early endosome is visualized as a discrete, bright yellow area in one cell (Fig. 2c). PKC β II redistribution

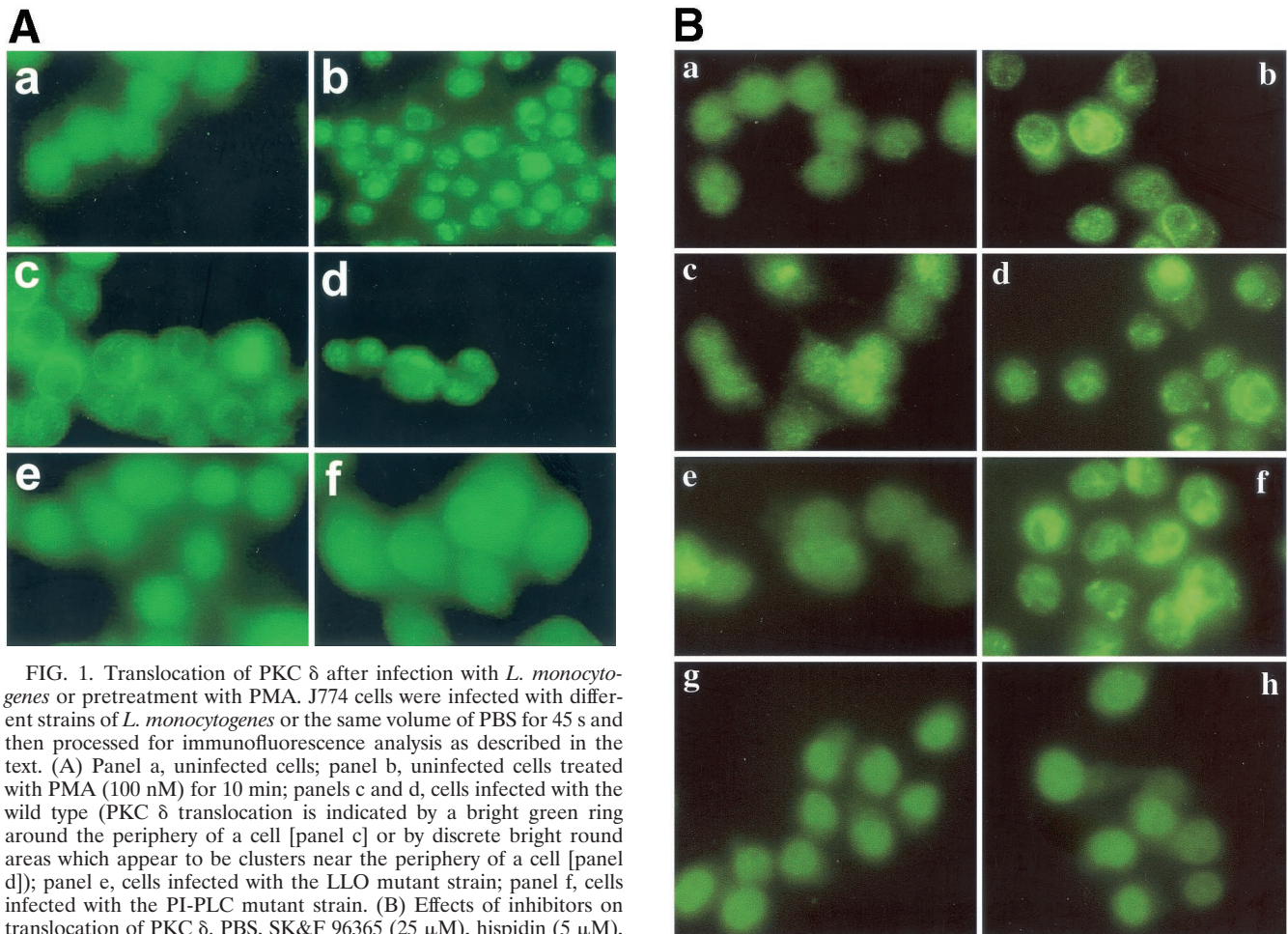


FIG. 1. Translocation of PKC δ after infection with *L. monocytogenes* or pretreatment with PMA. J774 cells were infected with different strains of *L. monocytogenes* or the same volume of PBS for 45 s and then processed for immunofluorescence analysis as described in the text. (A) Panel a, uninfected cells; panel b, uninfected cells treated with PMA (100 nM) for 10 min; panels c and d, cells infected with the wild type (PKC δ translocation is indicated by a bright green ring around the periphery of a cell [panel c] or by discrete bright round areas which appear to be clusters near the periphery of a cell [panel d]); panel e, cells infected with the LLO mutant strain; panel f, cells infected with the PI-PLC mutant strain. (B) Effects of inhibitors on translocation of PKC δ . PBS, SK&F 96365 (25 μ M), hispidin (5 μ M), or rottlerin (25 μ M) was added to J774 cells 30 min prior to infection with the wild type. Uninfected cells to which PBS or inhibitor was added 30 min prior to infection are shown in the left panel of each row. Control or inhibitor-treated cells infected with the wild type for 45 s are shown in the right panel of each row. Panels a and b, control; panels c and d, cells pretreated with SK&F 96365; panels e and f, cells pretreated with hispidin; panels g and h, cells pretreated with rottlerin.

to early endosomes occurred within 30 s after addition of the wild-type strain, and the results after 45 s are shown in Fig. 2d to f. Similar redistribution was seen with the BR-PLC mutant strain (data not shown). Redistribution was not observed after 1 min. Figure 2e shows that transferrin-labeled early endosomes are larger (1 to 6 μ m) than the bodies in uninfected cells and that their distribution is not mainly peripheral. In Fig. 2d several of these bodies are labeled with antibody to PKC β II, and in Fig. 2f they are colocalized as discrete yellow bodies. Infection with an LLO-deficient strain (Fig. 2g to i) or a PI-PLC-deficient strain (Fig. 2j to l) did not result in translocation of the PKC β II isoform, which suggests that PKC β II translocation depends on both LLO and PI-PLC. Some change in the distribution of transferrin-labeled early endosomes was observed upon infection with the LLO mutant (Fig. 2h), but these endosomes did not colocalize with PKC β II. An increase in the number of larger endosomes was also detected in cells infected with the BR-PLC and double phospholipase mutant

strains (data not shown). Increased size of early endosomes does not appear to be coupled to PKC β II translocation.

The results of immunofluorescence studies were confirmed by isolation of early endosomes, followed by Western blotting with antibody specific for PKC β II. Figure 3A shows that in uninfected cells there was some PKC β II in the early endosomes, but after 45 s of infection with the wild type or the BR-PLC mutant the amount of PKC β II was greatly increased. As was the case for immunofluorescence, this increase was not seen upon infection with the LLO, PI-PLC, or double phospholipase mutants.

(iv) **PKC β I translocation.** In uninfected cells some colocalization of PKC β I with transferrin-labeled early endosomes was observed; this occurred in $\leq 10\%$ of the cells (Fig. 4a to c). After infection with the wild type (Fig. 4d to f) or the PI-PLC mutant strain (Fig. 4g to i) noticeably more colocalization of PKC β I with early endosomes was observed within 4 min after addition of bacteria. As shown in Fig. 4, redistribution of transferrin-labeled early endosomes occurred after infection, resulting in larger, more centrally located bodies. Colocalization of PKC β I with early endosomes was also seen after infection with the BR-PLC or double phospholipase mutant strains (data not shown). By 5 min redistribution of PKC β I was no longer observed after infection with the wild type

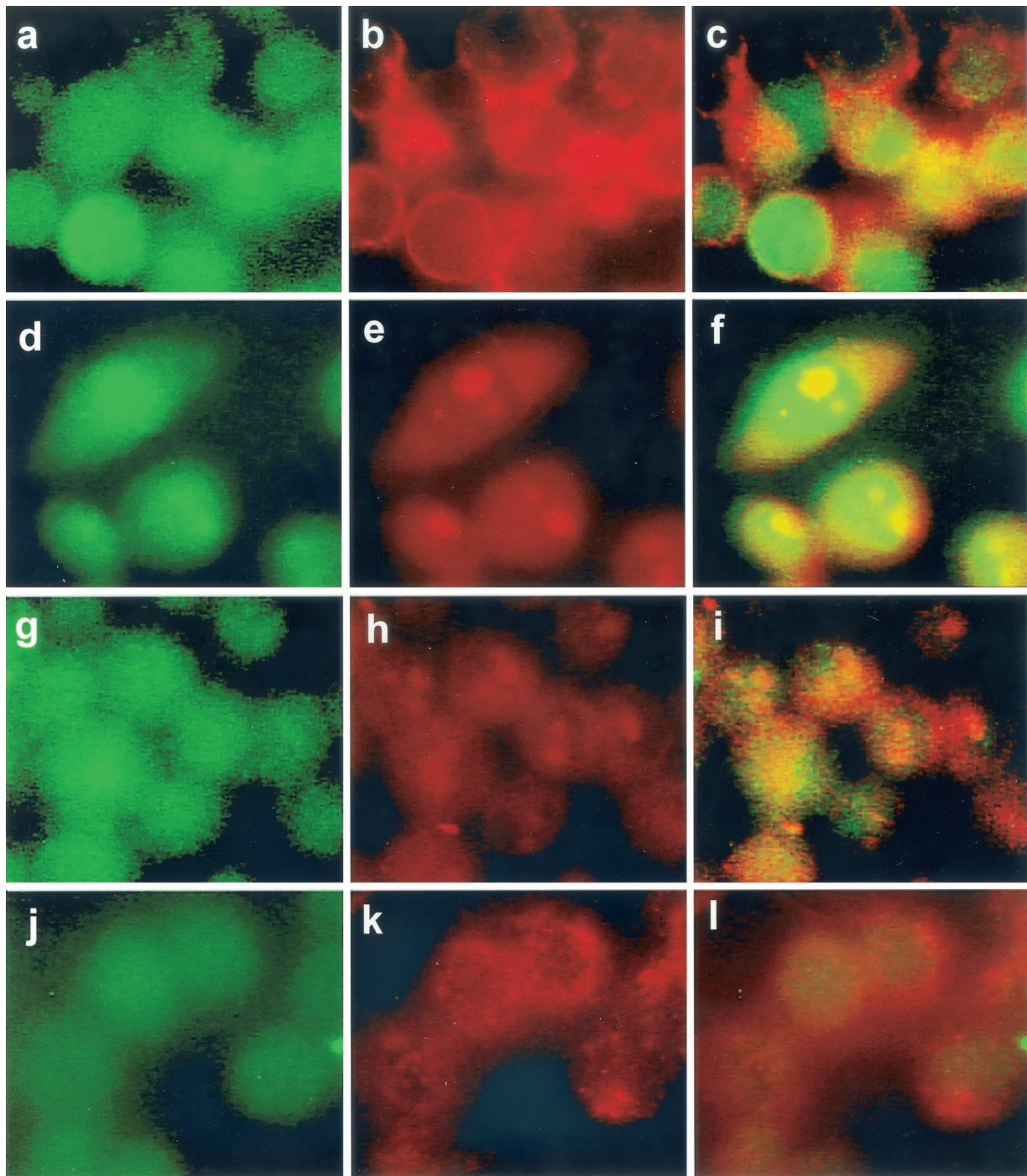


FIG. 2. Translocation of PKC β II to early endosomes of host J774 cells after infection with *L. monocytogenes*. PKC β II was labeled with FITC-conjugated secondary antibody as described in the text, and cells labeled for PKC β II are shown in the left panel of each row. Early endosomes labeled with rhodamine-conjugated transferrin are shown in the middle panel of each row. In uninfected cells these endosomes appear as discrete red areas near the periphery of a cell. In uninfected cells PKC β II is distributed throughout the cells and is also colocalized with early endosomes in $\leq 10\%$ of the cells. The right panel of each row is the merged left and middle panels obtained by using the Phase 3 Imaging software. Upon infection with the wild type, PKC β II translocation to the early endosomes 45 s after addition of the bacteria appears as bright, discrete yellow areas in the same location as the early endosomes (f). PKC β II translocation did not occur after infection with mutant strains lacking LLO (g to i) or PI-PLC (j to l).

(data not shown). Addition of the strain lacking LLO did not result in PKC β I translocation to early endosomes (Fig. 4j to l).

The results of immunofluorescence studies of PKC β I were

supported by isolation of early endosomes followed by Western blotting with antibody specific for PKC β I. Figure 5 shows that in uninfected cells there was some PKC β I at the early endosomes, but after infection with the wild type or the PI-

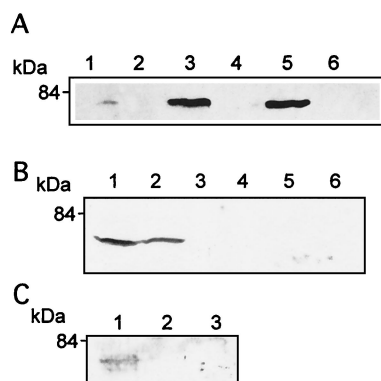


FIG. 3. Isolation of early endosomes and Western blotting revealed translocation of PKC β II after infection. J774 cells were infected with the wild type or mutant strains of *L. monocytogenes* for 45 s, and purified endosome fractions were prepared. One hundred micrograms of protein of each sample (from two pooled endosome preparations) was used for SDS-polyacrylamide gel electrophoresis. (A) Infection with the wild type (lane 3) and the BR-PLC mutant strain (lane 5) resulted in increased PKC β II compared to the PKC β II in the uninfected cells (lane 1). Translocation of PKC β II was not observed in cells infected with the double phospholipase mutant (lane 2), the PI-PLC mutant (lane 4), or the LLO mutant (lane 6). (B) SK&F 96365 and hispidin inhibit translocation of PKC β II after infection with the wild type or the BR-PLC mutant strain. J774 cells were infected with the wild type (lane 1) or the BR-PLC mutant (lane 2), pretreated for 30 min with SK&F 91635 (25 μ M) and infected with the wild type (lane 3) or the BR-PLC mutant (lane 4), or pretreated for 30 min with hispidin (5 μ M) and infected with the wild type (lane 5) or the BR-PLC mutant (lane 6). (C) Rottlerin inhibits translocation of PKC β II after infection with the wild type. J774 cells were infected with the wild type (lane 1), pretreated for 30 min with hispidin (5 μ M) and infected with wild type (lane 2), or pretreated for 30 min with rottlerin (25 μ M) and infected with the wild type (lane 3).

PLC mutant the amount of PKC β I was significantly greater. As determined by immunofluorescence, there was no translocation of PKC β I upon infection with the LLO mutant. The time course of translocation of PKC β I is shown in Fig. 6; it reached a maximum at 4 min and was essentially gone at 5 min.

(v) **Effects of inhibitors on PKC β I and PKC β II translocation.** The effects of the calcium channel blocker SK&F 96365 on translocation of both PKC β I and PKC β II were studied in order to determine calcium requirements for translocation of these molecules. The so-called classical isoforms of PKC, including PKC β , are activated by calcium and/or DAG (26). In J774 cells, 25 μ M SK&F 96365 did not prevent the translocation of PKC β I to early endosomes after infection with the wild type, which indicates that translocation of this isoform was independent of calcium influx (Fig. 5). However, PKC β II translocation after infection with the wild type or the BR-PLC mutant strain was inhibited in cells treated with SK&F 96365, indicating that translocation of this isoform requires the initial calcium influx observed at 1 min postinfection (35) (Fig. 3B).

In contrast, hispidin (5 μ M), the PKC β inhibitor, prevented translocation of both PKC β I (Fig. 5) and PKC β II (Fig. 3B) to early endosomes after infection with the wild type. At a concentration of 25 μ M, rottlerin, an inhibitor of PKC δ at concentrations lower than those required for inhibition of other PKC isoforms, did not affect translocation of PKC β I to

early endosomes (data not shown), but it did inhibit translocation of PKC β II to early endosomes, which indicates that PKC β II activation is downstream of PKC δ mobilization (Fig. 3C).

Effects of inhibitors on calcium signaling. Since wild-type *L. monocytogenes* and the strain lacking BR-PLC induce an influx of calcium within 1 min after addition of bacteria to cells (35) and rapid translocation of the calcium-independent PKC δ isoform and the classical PKC β isoforms, we tested the effects of the PKC δ inhibitor rottlerin on calcium signaling. In untreated cells the intracellular calcium concentration ($[Ca^{2+}]_i$) was elevated from 184 ± 34 to 501 ± 66 nM 1 min after infection with the wild type, as previously reported (35). In cells pretreated with 25 μ M rottlerin for 30 min, the initial calcium concentration after infection with the wild type was reduced to 273 ± 25 nM ($P < 0.05$, compared to the signal in untreated cells). Treatment of J774 cells with rottlerin prior to infection with the BR-PLC (*plcB*) mutant, which also produces the first increase in the calcium level (35), gave identical results (data not shown). Pretreatment with 5 μ M hispidin for 30 min resulted in no significant inhibition of the calcium signal after infection with the wild type (initial calcium concentration, 428 ± 34 nM).

Effects of hispidin on entry of *L. monocytogenes* into J774 cells. The results described above suggest that PKC δ translocation precedes the first increase in the calcium level and that both of these signals are required for PKC β II translocation. PKC δ activation requires DAG, which is provided by the action of *L. monocytogenes* PI-PLC on host PI in the presence of LLO (12). Accordingly, we propose the following signaling pathway: PI-PLC \rightarrow DAG \rightarrow PKC δ translocation \rightarrow elevated $[Ca^{2+}]_i \rightarrow$ PKC β II translocation. As was the case when the first increase in calcium level was prevented by treatment with SK&F 96365 (35), we found that the total number of wild-type bacteria associated with hispidin-treated J774 cells at 1 min was significantly higher than the number associated with untreated J774 cells (Fig. 7A).

Internalization of the wild type was also affected by hispidin treatment. The percentage of internalized wild-type *L. monocytogenes* cells was significantly higher in treated J774 cells than in untreated J774 cells (Fig. 7C). The percentage of internalized wild-type bacteria remained significantly elevated in hispidin-treated J774 cells until 20 min. There was a decline from $67\% \pm 2.9\%$ at 10 min to $38\% \pm 2.3\%$ at 20 min. This decline in part reflected the increased total number of bacteria associated with hispidin-treated cells at 20 min (Fig. 7A). Similar increases in internalization of the BR-PLC mutant were also seen after treatment with hispidin (data not shown). While these results suggest a role for PKC β activation in controlling entry of the wild type at very early time points, they do not distinguish between the PKC β I and PKC β II isoforms.

Since hispidin affects both PKC β I and PKC β II translocation and since the PI-PLC mutant activates only PKC β I, we tested the effects of hispidin on the entry kinetics of this strain to determine if PKC β I translocation has a role in controlling entry of *L. monocytogenes*. We found that hispidin did not have a significant effect on the total number of cells of this strain associated with J774 cells (Fig. 7B). Entry of the PI-PLC mutant strain into hispidin-treated cells was also not significantly different from entry into untreated cells during the 20-min

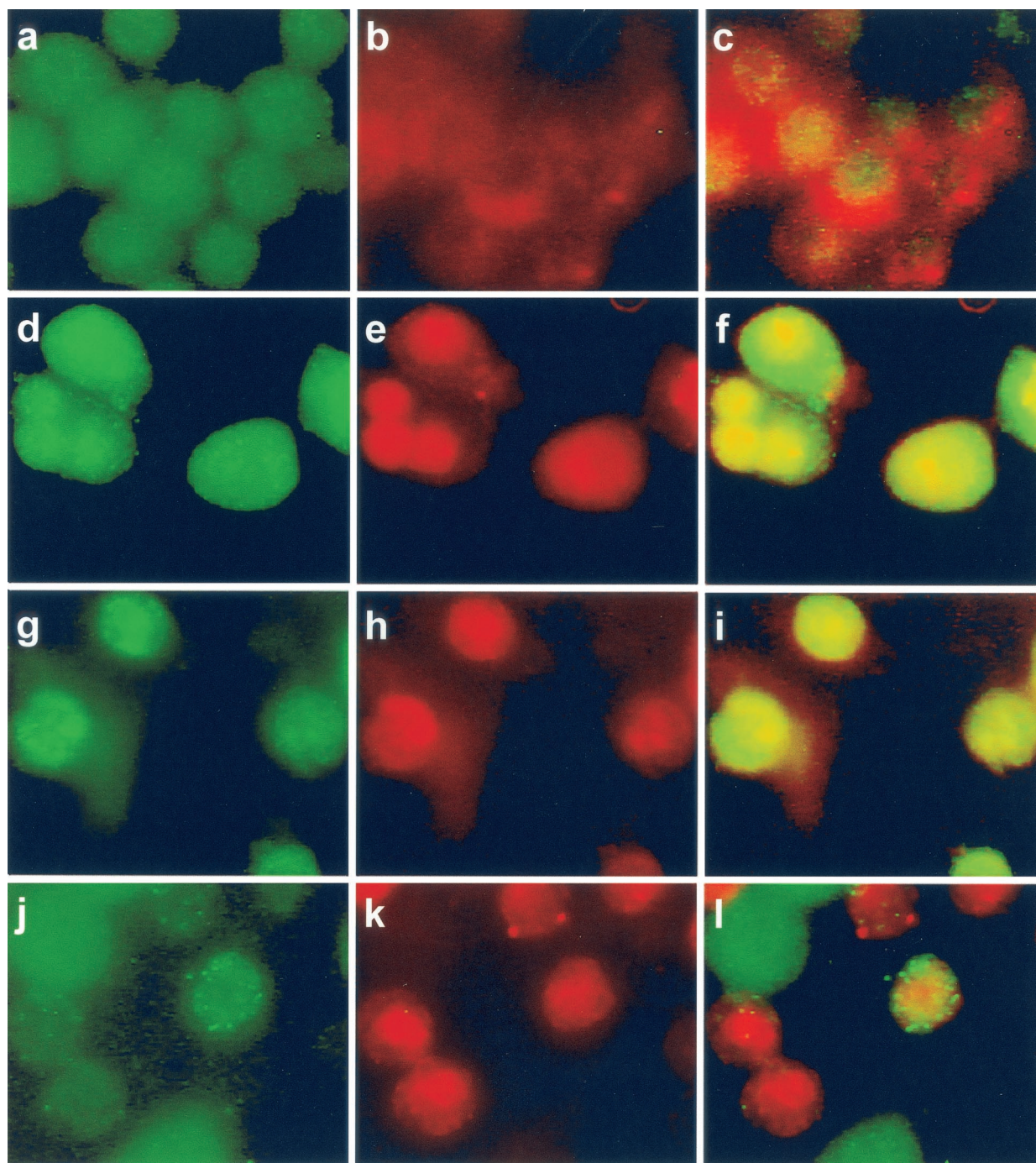


FIG. 4. PKC β I translocation occurred after infection with the wild type or the PI-PLC mutant strain but not after infection with the LLO mutant strain. PKC β I was labeled with FITC-conjugated secondary antibody as described in the text, and cells labeled for PKC β I are shown in the left panel of each row. Early endosomes were labeled with rhodamine-conjugated transferrin and appear in the middle panel of each row as discrete red areas. In uninfected cells PKC β I was located throughout the cytosol, could also appear as a discrete green area around the periphery of a cell, and could be colocalized with early endosomes. Cells were infected with the strains for 4 min. PKC β I translocation after infection with the wild-type strain (d to f) or the PI-PLC mutant strain (g to i) appears as discrete bright yellow areas corresponding to PKC β I colocalization with transferrin-labeled early endosomes. The images in the right panels were obtained as described in the legend to Fig. 2. Cells infected with the strain lacking LLO did not show translocation of PKC β I to early endosomes (j to l). Bright green objects seen especially in panels j and l are FITC-labeled bacteria.

infection period (Fig. 7D). These results, which suggest that both PKC β I and PKC β II control the entry of *L. monocytogenes* into J774 cells, are discussed below.

Effects of lipidin on escape from the primary vacuole.

When J774 cells were treated with the calcium signal inhibitors SK&F 96365 and thapsigargin and infected with wild-type *L. monocytogenes*, the percentage of internalized bacteria that escaped from the primary vacuole decreased from 44% to 14

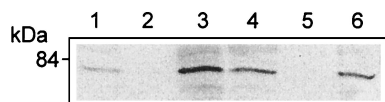


FIG. 5. Isolation of early endosomes and Western blotting revealed translocation of PKC β I after infection. J774 cells were infected with wild-type or mutant *L. monocytogenes* for 4 min, and purified endosome fractions were prepared. One hundred micrograms of protein of each sample (from two pooled endosome preparations) was used for SDS-polyacrylamide gel electrophoresis followed by Western blotting, as described in the text. PKC β I translocation was observed in cells infected with the wild type (lane 3) and the PI-PLC mutant (lane 6) compared to uninfected cells (lane 1). Translocation was not seen after infection with the LLO mutant (lane 2) or after 30 min of pretreatment with hispidin and infection with the wild type (lane 5). Cells pretreated with SK&F 96365 for 30 min showed translocation of PKC β I (lane 4).

and 21%, respectively (35). These results suggested that calcium signaling affected the ability of *L. monocytogenes* to leave the primary phagosome. Since calcium signaling is required for translocation of PKC β II to early endosomes, we examined the effects of inhibition of PKC β translocation by hispidin on escape. Like SK&F 96365, hispidin reduced the percentage of wild-type bacteria that escaped at 1.5 h after infection from 43 to 15% (Fig. 8A). The ability of the PI-PLC mutant to escape from the primary vacuole is significantly impaired compared to the ability of the wild type (5, 30). When J774 cells were treated with hispidin and infected with the PI-PLC mutant, in which PKC β I but not PKC β II was translocated to early endosomes, the percentage of bacteria that escaped was markedly reduced (from 23 to 4.5%) (Fig. 8B), suggesting an important role for PKC β I in determining eventual escape from the primary phagocytic vacuole.

DISCUSSION

The observation that elevations in cytosolic calcium levels occurred 1 and 5 min after infection of J774 cells with wild-type *L. monocytogenes* (35) and the finding that PKC δ and PKC β isoforms were translocated within the first 5 min after infection formed the basis for the present study, in which we examined the relationships among cytosolic calcium, bacterial phospholipase activities, and host PKC activation. We present evidence that there is coupling of PKC δ , calcium signaling, and PKC β II translocation in J774 cells after infection with *L. monocytogenes* and demonstrate that pharmacological inhibition of calcium signals disrupts the signaling pathway. We also dem-

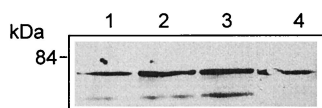


FIG. 6. Time course of translocation of PKC β I to early endosomes. Cells were infected with the wild type and harvested at intervals after infection. Early endosomes were isolated, and proteins were prepared for SDS-polyacrylamide gel electrophoresis and Western blotting as described in Materials and Methods. The proteins were also blotted with antibody to the transferrin receptor (upper bands). Infections were carried out for 1 min (lane 1), 3 min (lane 2), 4 min (lane 3), and 5 min (lane 4).

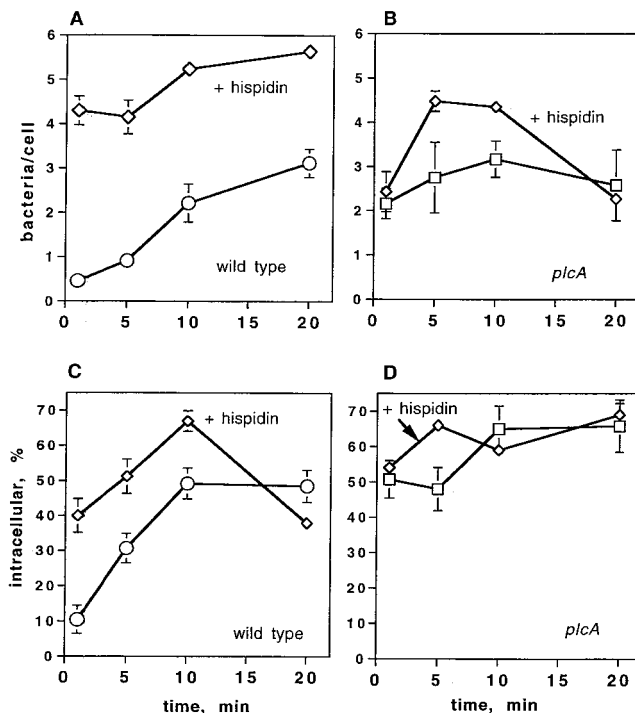


FIG. 7. Effects of hispidin on association of *L. monocytogenes* with J774 cells and entry of *L. monocytogenes* into J774 cells. (A) Association of the wild type with untreated J774 cells (\circ) or cells pretreated with hispidin ($5 \mu\text{M}$) (\diamond). (B) Association of the PI-PLC mutant with untreated J774 cells (\square) or cells pretreated with hispidin ($5 \mu\text{M}$) (\diamond). (C) Percentage of associated wild-type bacteria that were internalized in untreated J774 cells (\circ) or cells pretreated with hispidin ($5 \mu\text{M}$) (\diamond). (D) Percentage of associated PI-PLC mutant bacteria that were internalized in untreated J774 cells (\square) or cells pretreated for 30 min with hispidin ($5 \mu\text{M}$) (\diamond). The total number of bacteria associated with the J774 cells was calculated as follows: total number of FITC-labeled bacteria (green)/total number of cells per image. The results are expressed as averages \pm standard errors of the means for three sets of experiments in which a total of 200 to 250 J774 cells were counted. For association of the wild type in cells treated with hispidin $P < 0.05$ at 1, 5, and 10 min compared to the association for untreated cells. The percentage of internalized bacteria was calculated as described in the text. The results are expressed as averages \pm standard errors of the means for three sets of experiments in which a total of 200 to 250 J774 cells were counted. For the percentage of internalized wild-type bacteria in cells treated with hispidin $P < 0.05$ compared to the percentage for untreated cells at 1, 5, and 10 min.

onstrate that an apparently calcium-independent but LLO-dependent translocation of PKC β I occurs.

The observation that PKC δ translocates to the cell periphery by 30 s after infection is consistent with our previous hypothesis that it plays a role in the influx of calcium from the extracellular fluid that was observed to peak at 1 min after infection (35). Treatment with rottlerin, a relatively specific PKC δ inhibitor, resulted in significant inhibition of calcium signaling. Although recent work indicates that rottlerin may act as a mitochondrial uncoupler which reduces ATP levels (31), the specific effects of this compound on PKC δ and PKC β II, but not on PKC β I translocation, are consistent with a pathway from PKC δ to PKC β II. Inhibition of calcium entry with the channel blocker SK&F 96365 did not prevent PKC δ translocation, whereas presumed inhibition of PKC activation by 3 h

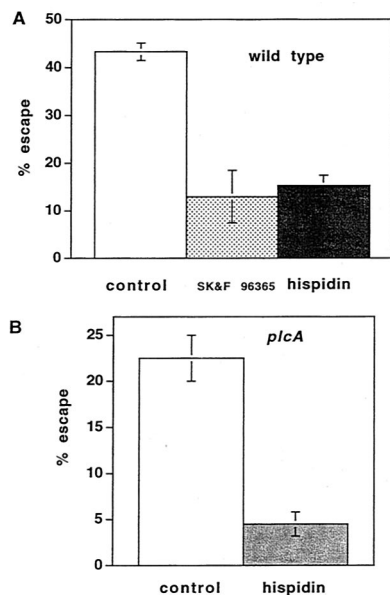


FIG. 8. Hispidin pretreatment inhibited escape of the wild type and the PI-PLC mutant from the phagosome. Bacteria that escape from the phagosome and enter the cytosol become decorated with polymerized actin and can be stained with fluorescent phalloidin. After removal of uninternalized bacteria with gentamicin at 30 min, the percentage of cells that escaped at 1.5 h after infection was calculated as described in Materials and Methods. (A) Cells were either not pretreated (control) or pretreated with hispidin (5 μ M) for 30 min and infected with the wild type. The data are the averages \pm standard errors of the means for three experiments, and the difference is highly significant ($P < 0.001$). The data for cells pretreated with SK&F 96365 are taken from a previous study, in which the control gave an identical value (35). (B) Cells were pretreated with hispidin (5 μ M) for 30 min and infected with the PI-PLC mutant. The data are averages \pm standard errors of the means for three experiments, and the difference is highly significant ($P < 0.01$).

of pretreatment with PMA prevented the initial increase in $[Ca^{2+}]_i$ (data not shown). PKC δ has been shown to be involved in opening plasma membrane calcium channels (20, 34).

Based on these findings, we propose the following model for the coupling of intracellular calcium and PKC activation. Translocation of PKC δ to the periphery of the cell occurs upon addition of wild-type *L. monocytogenes* or the BR-PLC mutant strain but not upon addition of mutants with mutations in PI-PLC or LLO genes, which indicates that there is a requirement for at least two bacterial proteins, LLO and PI-PLC. Presumably, the combined activity of these proteins leads to hydrolysis of host PI and the formation of DAG (12, 27). We propose that this is responsible for the translocation of PKC δ , a calcium-independent isoform, and the subsequent initial elevation of intracellular calcium levels (Fig. 9), although a direct connection between PKC δ translocation and opening of the calcium channel has not been formally demonstrated.

Translocation of PKC β II to early endosomes of J774 cells also began within 30 s after addition of *L. monocytogenes*. This required both LLO and PI-PLC and was also inhibited by rottlerin and the calcium channel blocker SK&F 96365. Thus, translocation of this isoform appears to be coupled to PKC δ translocation and calcium signaling. In contrast to PKC β II translocation, PKC β I translocation to the early endosomes

occurred after infection with all of the strains tested except the strain lacking LLO. Since no calcium signaling was observed with the double phospholipase mutant (35), it appears that LLO is responsible for initiating a pulse of DAG, which in this case appears to be sufficient for PKC β I translocation (26). Consistent with this is our finding that the double phospholipase mutant, but not the LLO mutant strain, activates host polyphosphoinositide-specific PLC (12). PKC β I translocation was not inhibited by SK&F 96365, also indicating that elevation of the calcium level is not required for PKC β I translocation to early endosomes. Translocation of PKC β I and PKC β II to early endosomes has not been reported previously.

The PI-PLC and the double phospholipase deletion strains, which mobilize PKC β I but not PKC β II or PKC δ , demonstrated higher early association with J774 cells and more rapid entry than strains that mobilize all three PKC isoforms (Fig. 7). We suggest, therefore, that PKC β I activation permits earlier and more rapid bacterial entry and that PKC β II activation appears to modify this effect by temporarily slowing bacterial entry. When neither PKC β I nor PKC β II is translocated, as is the case with a mutant with a mutation in the LLO gene or with heat-killed bacteria, uptake is also rapid (35), suggesting that this rate is the rate for particles that bind to surface receptors and are unable to modify the host response. In a recent study, translocation of two nonclassical PKC isoforms, PKC δ and PKC ϵ , was associated with uptake of opsonized particles into RAW 264.7 cells via the Fc γ receptor (19). These studies and those reported here suggest that PKC δ translocation and downstream events may play a role in both Fc γ receptor-mediated and Fc γ receptor-independent uptake.

As shown in Fig. 8, inhibition of PKC β translocation by hispidin had dramatic effects on the ability of both wild-type and PI-PLC mutant bacteria to escape from the primary vacuole. During infection of J774 cells with the wild type, 43% of

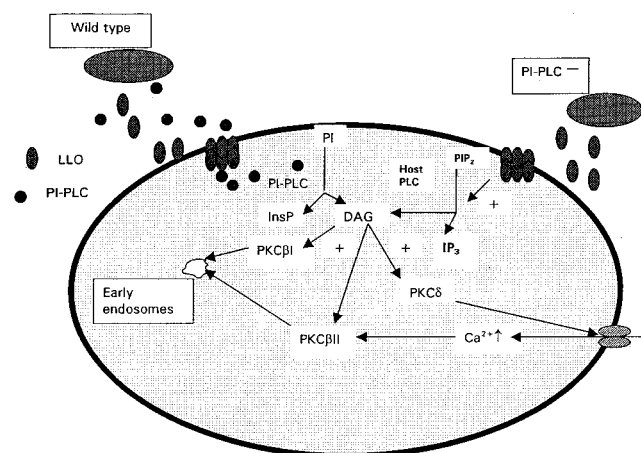


FIG. 9. Suggested model for coupling of PKC activation and calcium signaling in host J774 cells after infection with *L. monocytogenes*. As described in the text, we suggest that PKC δ , calcium influx, and PKC β II activation are coupled and are initiated as a result of activity of two listerial proteins, LLO and PI-PLC. Activation of PKC β I did not require PI-PLC or elevated $[Ca^{2+}]_i$, and we suggest that it occurs as a result of the formation of DAG as a result of the action of host PLC on phosphatidylinositol 4,5-bisphosphate (PIP₂) (12), yielding inositol 1,4,5-triphosphate (IP₃).

the internalized bacteria had escaped from the primary vacuole at 1.5 h after infection. When cells were pretreated with the calcium channel blocker SK&F 96365, which blocked all calcium signaling, and with thapsigargin, which emptied cellular calcium stores and blocked the second and third calcium signals, the ability of the wild type to escape was reduced to 14 and 21%, respectively (35). Since blockage of the calcium signals inhibited PKC β II translocation, we tested the effects of hispidin, which blocked PKC β I and PKC β II translocation, on escape from the primary vacuole and observed that escape was reduced from 43 to 15%, paralleling the results obtained with inhibitors of calcium signaling. Infection of J774 cells with the mutant with a deletion in the PI-PLC gene resulted in translocation of PKC β I but not translocation of PKC β II. When cells were treated with hispidin and infected with the PI-PLC mutant, escape was reduced from 23 to 4.5% (Fig. 8B). These results strongly suggest that PKC signaling has a profound effect on later events during an infection. In order to determine if PKC signals in addition to those observed during the initial stages of infection are required, we performed experiments in which hispidin was removed from the medium 5 and 15 min after infection with the wild type. We observed that washing the cells at these times, which were earlier than the normal wash time (30 min), resulted in escape of fewer bacteria into the cytosol than usually observed (27 versus 38% in these experiments). When hispidin was removed at either 5 or 15 min after infection, the percentage of bacteria that escaped into the cytosol did not differ from the percentage in controls to which hispidin had not been added (data not shown). These results suggest that PKC β signaling after internalization plays a role in the ability of *L. monocytogenes* to exit the primary vacuole.

The finding that early endosomes enlarge upon infection with the wild type (Fig. 2 and 4) is intriguing and deserves further study. Rab5 is thought to play an important role in regulating early-endosome fusion, and large endosomes thought to arise from fusion have been associated with overexpression of Rab5 or expression of the GTPase mutant Rab5: Q79L (3, 21, 32). In an *in vitro* system, phagosomes containing live LLO⁻*L. monocytogenes* recruited Rab5 faster than phagosomes containing dead bacteria recruited Rab5 (1).

Generation of the host signals appears to be coupled to specific bacterial proteins, and thus *L. monocytogenes* is able to manipulate host signaling mechanisms to ensure its own survival. These studies, along with our previous work on calcium signaling in J774 cells (35) and studies of endothelial cells (27, 28) and neutrophils (29), draw additional attention to the engagement of secreted proteins, such as LLO and the two phospholipases, with host cells prior to uptake of the bacteria. Recent work with the extracellular pathogen *Streptococcus pyogenes* demonstrated a role for streptolysin O, a member of the same family of cholesterol-dependent cytolysins as LLO, in permitting the entry of a bacterial protein into the host cell, analogous to the type III secretion system of gram-negative bacteria (22). A similar model was proposed for LLO and PI-PLC (27), and the present results and previous results (35) support such a model (Fig. 9). Expression of both LLO and PI-PLC is increased upon entry of *L. monocytogenes* into the phagocytic vacuole (2, 16, 24). Distinguishing between the effects of these proteins before and after entry into the host cell

on the fate of *L. monocytogenes* in a macrophage will undoubtedly be the focus of considerable effort in the future.

ACKNOWLEDGMENTS

This work was supported by Public Health Service grants GM 52797 and AI 45153 (to H.G.) and by the University of Pennsylvania Research Foundation.

REFERENCES

1. Alvarez-Dominguez, C., A. M. Barbieri, W. Berón, A. Wandinger-Ness, and P. D. Stahl. 1996. Phagocytosed live *Listeria monocytogenes* influences rab5-regulated *in vitro* phagosome-endosome fusion. *J. Biol. Chem.* **271**:13834–13843.
2. Bubert, A., Z. Sokolovic, S. K. Chun, L. Papatheodorou, A. Simm, and W. Goebel. 1999. Differential expression of *Listeria monocytogenes* virulence genes in mammalian host cells. *Mol. Gen. Genet.* **261**:323–336.
3. Bucci, C., R. G. Parton, I. H. Mather, H. Stunnenberg, K. Simons, B. Hoffack, and M. Zerial. 1992. The small GTPase rab5 functions as a regulatory factor in the early endocytic pathway. *Cell* **70**:715–728.
4. Camilli, A., H. Goldfine, and D. A. Portnoy. 1991. *Listeria monocytogenes* mutants lacking phosphatidylinositol-specific phospholipase C are avirulent. *J. Exp. Med.* **173**:751–754.
5. Camilli, A., L. G. Tilney, and D. A. Portnoy. 1993. Dual roles of *plcA* in *Listeria monocytogenes* pathogenesis. *Mol. Microbiol.* **8**:143–157.
6. Claus, V., A. Jahraus, T. Tjelle, T. Berg, H. Kirschke, H. Faulstich, and G. Griffiths. 1998. Lysosomal enzyme trafficking between phagosomes, endosomes, and lysosomes in J774 macrophages—enrichment of cathepsin H in early endosomes. *J. Biol. Chem.* **273**:9842–9851.
7. Diaz, R., L. Mayorga, and P. Stahl. 1988. *In vitro* fusion of endosomes following receptor-mediated endocytosis. *J. Biol. Chem.* **263**:6093–6100.
8. Drevets, D. A., and P. A. Campbell. 1991. Macrophage phagocytosis: use of fluorescence microscopy to distinguish between extracellular and intracellular bacteria. *J. Immunol. Methods* **142**:31–38.
9. Findlay, J., G. A. Levy, and C. A. Marsh. 1958. Inhibition of glycosidases by aldono-lactones of corresponding configuration. *Biochem. J.* **69**:467–476.
10. Geoffroy, C., J. Raveneau, J.-L. Beretti, A. Lecroisey, J.-A. Vazquez-Boland, J. E. Alouf, and P. Berche. 1991. Purification and characterization of an extracellular 29-kilodalton phospholipase C from *Listeria monocytogenes*. *Infect. Immun.* **59**:2382–2388.
11. Goldfine, H., N. C. Johnston, and C. Knob. 1993. The nonspecific phospholipase C of *Listeria monocytogenes*: activity on phospholipids in Triton X-100 mixed micelles and in biological membranes. *J. Bacteriol.* **175**:4298–4306.
12. Goldfine, H., S. J. Wadsworth, and N. C. Johnston. 2000. Activation of host phospholipases C and D in macrophages after infection with *Listeria monocytogenes*. *Infect. Immun.* **68**:5735–5741.
13. Gonindard, C., C. Bergonzi, C. Denier, C. Sergheraert, A. Klæbe, L. Chavant, and E. Hollande. 1997. Synthetic hispidin, a PKC inhibitor, is more cytotoxic toward cancer cells than normal cells *in vitro*. *Cell Biol. Toxicol.* **13**:141–153.
14. Gschwendt, M., H. J. Muller, K. Kielbassa, R. Zang, W. Kittstein, G. Rincke, and E. Marks. 1994. Rottlerin, a novel protein kinase inhibitor. *Biochem. Biophys. Res. Commun.* **199**:93–98.
15. Jones, S., and D. A. Portnoy. 1994. Characterization of *Listeria monocytogenes* pathogenesis in a strain expressing perfringolysin O in place of listeriolysin O. *Infect. Immun.* **62**:5608–5613.
16. Klarsfeld, A. D., P. L. Goossens, and P. Cossart. 1994. Five *Listeria monocytogenes* genes preferentially expressed in infected mammalian cells: *plcA*, *purH*, *purD*, *pyrE* and an arginine ABC transporter gene, *arpJ*. *Mol. Microbiol.* **13**:585–597.
17. Kontny, E., M. Kurowska, K. Szczepanska, and W. Maslinski. 2000. Rottlerin, a PKC isozyme-selective inhibitor, affects signaling events and cytokine production in human monocytes. *J. Leukoc. Biol.* **67**:249–258.
18. Lang, T., and C. De Chastellier. 1985. Fluid phase and mannose receptor-mediated uptake of horseradish peroxidase in mouse bone marrow-derived macrophages. Biochemical and ultrastructural study. *Biol. Cell* **53**:149–154.
19. Larsen, E. C., J. A. DiGennaro, N. Saito, S. Mehta, D. J. Loegering, J. E. Mazurkiewicz, and M. R. Lennartz. 2000. Differential requirement for classic and novel PKC isoforms in respiratory burst and phagocytosis in RAW 264.7 cells. *J. Immunol.* **165**:2809–2817.
20. Levin, R., A. Braiman, and Z. Priel. 1997. Protein kinase C induced calcium influx and sustained enhancement of ciliary beating by extracellular ATP. *Cell Calcium* **21**:103–113.
21. Li, G., M. A. Barbieri, M. I. Colombo, and P. D. Stahl. 1994. Structural features of the GTP-binding defective Rab5 mutants required for their inhibitory activity on endocytosis. *J. Biol. Chem.* **269**:14631–14635.
22. Madden, J. C., N. Ruiz, and M. Caparon. 2001. Cytolysin-mediated translocation (CMT): a functional equivalent of type III secretion in Gram-positive bacteria. *Cell* **104**:143–152.
23. Mengaud, J., C. Braun-Breton, and P. Cossart. 1991. Identification of phos-

- phatidylinositol-specific phospholipase C activity in *Listeria monocytogenes*: a novel type of virulence factor. *Mol. Microbiol.* **5**:367–372.
24. **Moors, M. A., B. Levitt, P. Youngman, and D. A. Portnoy.** 1999. Expression of listeriolysin O and ActA by intracellular and extracellular *Listeria monocytogenes*. *Infect. Immun.* **67**:131–139.
 25. **Portnoy, D. A., P. S. Jacks, and D. J. Hinrichs.** 1988. Role of hemolysin for the intracellular growth of *Listeria monocytogenes*. *J. Exp. Med.* **167**:1459–1471.
 26. **Ron, D., and M. G. Kazanietz.** 1999. New insights into the regulation of protein kinase C and novel phorbol ester receptors. *FASEB J.* **13**:1658–1676.
 27. **Sibeliuss, U., T. Chakraborty, B. Krögel, J. Wolf, F. Rose, R. Schmidt, J. Wehland, W. Seeger, and F. Grimminger.** 1996. The listerial exotoxins listeriolysin and phosphatidylinositol-specific phospholipase C synergize to elicit endothelial cell phosphoinositide metabolism. *J. Immunol.* **157**:4055–4060.
 28. **Sibeliuss, U., F. Rose, T. Chakraborty, A. Darji, J. Wehland, S. Weiss, W. Seeger, and F. Grimminger.** 1996. Listeriolysin is a potent inducer of the phosphatidylinositol response and lipid mediator generation in human endothelial cells. *Infect. Immun.* **64**:674–676.
 29. **Sibeliuss, U., E. C. Schulz, F. Rose, K. Hattar, T. Jacobs, S. Weiss, T. Chakraborty, W. Seeger, and F. Grimminger.** 1999. Role of *Listeria monocytogenes* exotoxins listeriolysin and phosphatidylinositol-specific phospholipase C in activation of human neutrophils. *Infect. Immun.* **67**:1125–1130.
 30. **Smith, G. A., H. Marquis, S. Jones, N. C. Johnston, D. A. Portnoy, and H. Goldfine.** 1995. The two distinct phospholipases C of *Listeria monocytogenes* have overlapping roles in escape from a vacuole and cell-to-cell spread. *Infect. Immun.* **63**:4231–4237.
 31. **Soltoff, S. P.** 2001. Rottlerin is a mitochondrial uncoupler that decreases cellular ATP levels and indirectly blocks protein kinase C δ tyrosine phosphorylation. *J. Biol. Chem.* **276**:37986–37992.
 32. **Stenmark, H., R. G. Parton, O. Steele-Mortimer, A. Lutcke, J. Gruenberg, and M. Zerial.** 1994. Inhibition of rab5 GTPase activity stimulates membrane fusion in endocytosis. *EMBO J.* **13**:1287–1296.
 33. **Tilney, L. G., and D. A. Portnoy.** 1989. Actin filaments and the growth, movement, and spread of the intracellular bacterial parasite *Listeria monocytogenes*. *J. Cell Biol.* **109**:1597–1608.
 34. **Vazquez, G., and A. R. de Boland.** 1996. Involvement of protein kinase C in the modulation of 1 α ,25-dihydroxy-vitamin D3-induced ⁴⁵Ca²⁺ uptake in rat and chick cultured myoblasts. *Biochim. Biophys. Acta* **1310**:157–162.
 35. **Wadsworth, S. J., and H. Goldfine.** 1999. *Listeria monocytogenes* phospholipase C-dependent calcium signaling modulates bacterial entry into J774 macrophage-like cells. *Infect. Immun.* **67**:1770–1778.

Editor: E. I. Tuomanen